Starfish-inspired Ultrasound Ciliary Bands for Microrobotic Systems

Cornel Dillinger, Nitesh Nama, and Daniel Ahmed

***Abstract*— Cilia are short, hair-like appendages ubiquitous in various biological systems, which have evolved to manipulate and gather food in liquids at regimes where viscosity dominates inertia. Inspired by these natural systems, synthetic cilia have been developed and cleverly utilized in microfluidics and microrobotics, to achieve functionalities such as propulsion, liquid pumping and mixing, and particle manipulation. In this article, we present the demonstration of soft ultrasound-activated synthetic ciliary bands that mimic the natural arrangements of ciliary bands on the surface of starfish larva.**

***Index Terms*— Acoustics, Bioinspired, Cilia, Propulsion, Soft robot application**

I. INTRODUCTION

CILIA can be found on the surfaces of many organisms, including algae and invertebrate larvae, which are naturally evolved to manipulate and gather food in liquids, where viscosity dominates inertia. Recent studies on the larval stages of marine invertebrates, such as starfish, have elicited that these invertebrates can adjust the orientation of cilia in their ciliary bands to control the direction of liquid flow; i.e. an analogous fluid source and sink are developed for their propulsion and feeding mechanisms [1]. Inspired by nature's cilia and their functions, engineered synthetic cilia and ciliary bands are of great interest for lab-on-chip devices and microrobotic systems. In particular, they promise solutions for many fundamental functions including propulsion, liquid pumping and mixing, and particle manipulation– all difficult to realize at microscale due to a lack of inertia [2][3]. Our system leverages nonlinear acoustics at microscales to drive bulk fluid motion via acoustically actuated small-amplitude oscillations of synthetic and soft cilia. By arranging the planar ciliary bands angled towards (+) or away (–) from each other, we achieve bulk fluid motion akin to a flow source or sink. We further combine these flow characteristics with a novel physical principle to circumvent the scallop theorem and realize acoustic-based propulsion and microparticle transport at microscales, by mimicking the feeding mechanism of starfish larva.

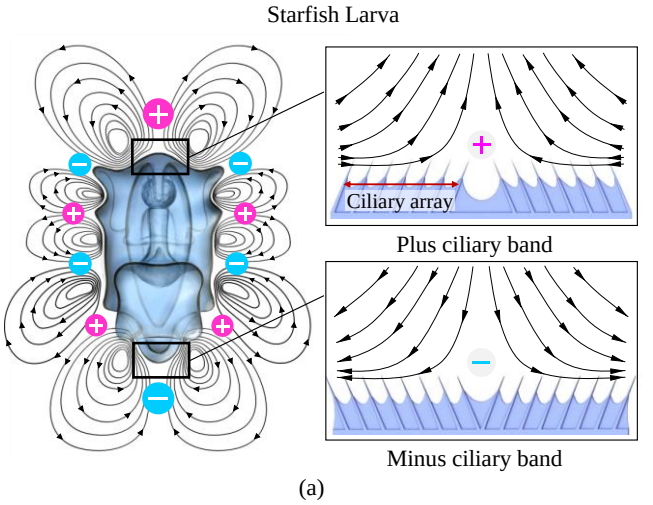

Fig. 1. Starfish larva-inspired ultrasound ciliary band designs. (a) Complex flow profile of counter-rotating vortices generated by a series of + and − ciliary bands. (b) Average velocities of + (top) and – (bottom) ciliary bands at sites indicated by magenta boxes versus voltage applied on the function generator. Scale bars, 100 µm.

This work has been supported by the European Research Council Starting Grant (SONOBOTS), Grant agreement No. 853309 and ETH Research Grant ETH-08 20-1 *(Corresponding author: Daniel Ahmed).*
Cornel Dillinger and Daniel Ahmed are with the Department of Mechanical and Process Engineering, ETH Zurich, Zurich, Switzerland (e-mail: corneld@ethz.ch; dahmed@ethz.ch).

Nitesh Nama is with Department of Mechanical and Materials Engineering, University of Nebraska-Lincoln, Lincoln, USA. (e-mail: nitesh.nama@unl.edu).

II. Results

A. Bioinspired Ciliary Bands

Inspired by the remarkable natural arrangements of ciliary bands on the surface of invertebrate larvae, we developed new designs for ultrasound-based soft ciliary bands that leverage the same physical principles (Fig. 1). To validate our concept, we fabricated "+" and "–" arrangements of cilia using ultraviolet (UV) photopolymerization method and performed experiments to characterize their behavior in an acoustic field. The UV photopolymerization method was developed under an inverted microscope. In short, masks containing the ciliary band designs were placed at the field stop of the microscope. UV light passes through a 20x objective and polymerized the polyethylene glycol and photoinitiator solution sandwiched between two glass slides. The fabricated + and – ciliary bands were comprised of two to eight soft cilia on each side. Each cilium had a length, base thickness, and height of L≈100 µm, W≈15 - 35 µm, and H≈50 µm, respectively, and as a set were arranged in series with separation of 20-40 µm. After fabrication, the ciliary bands were placed in an acoustic chamber filled with liquid solution containing tracer particles. A piezo transducer, which generated the acoustic field, was bonded next to the acoustic chamber and connected to an electronic function generator. The entire setup was mounted on an inverted microscope, and experimental results were captured using light-sensitive and high-speed cameras.

Over the course of the experiment, the acoustic field's excitation frequency was modulated from 20 - 100 kHz while maintaining an applied peak-to-peak voltage (Vpp) of 1-25. When exposed to such an acoustic field, the soft ciliary band undergoes small-amplitude oscillations, which result in a time-averaged steady flow field characterized by a pair of counter-rotating vortices in the surrounding liquid, also referred as acoustic streaming [4]. This acoustic streaming is driven by the dissipation of acoustic energy flux inside the fluid system that occurs, in general, both within and outside of the viscous boundary layer. However, for devices where the characteristic dimensions are much smaller compared to the acoustic wavelength, the acoustic streaming is primarily driven by the viscous dissipations within the boundary layer [5]. For the cilia system considered in this work, the thickness of viscous boundary layer can be computed as $\delta = \sqrt{(\nu/(\pi f))} = \sim 1.8 - 4.0$ µm , where $\nu \approx 10^{-6}$ m^2/s is the kinematic viscosity of water at room temperature, and f = 20 – 100 kHz is the excitation frequency. The viscous dissipations in this thin boundary layer drive the outer bulk streaming motion. This streaming profile is determined by the arrangement of the ciliary array relative to the normal axis of the underlying bulk surface. Referring to Fig. 1(b) (top), a + ciliary band comprises a pair of ciliary arrays that face each other and causes the liquid to flow away on a plane perpendicular to the center of the ciliary band, analogous to a fluid source. Conversely, in Fig. 1(b) (bottom) a – ciliary band consists of two ciliary arrays oriented away from each other and directs the streamline analogous to a fluid sink.

The strength of the flow produced from + and – ultrasound ciliary bands is determined by the intensity of the ambient acoustic field, which is controlled by adjusting the voltage applied to the piezoelectric transducer. Specifically, the streaming is driven by force and mass sources that depend quadratically on the first-order pressure and velocity of the governing Navier-Stokes equations, which in turn, depend linearly on the applied displacement amplitude introduced by the vibrations of the piezoelectric transducer [16]. Consequently, the streaming is expected to scale quadratically with the applied voltage (i.e., streaming velocity $\propto Vpp^2$). To investigate this scaling, we employed particle image velocimetry (PIV) to measure the average velocities normal to the ciliary bands at sites indicated by magenta boxes in Fig. 1b. The corresponding velocity data plots demonstrate the quadratic relation is reasonably well satisfied by the ciliary bands.

B. Bioinspired Microrobot

In this section, we analyze the swimming motion of a bioinspired, i.e. starfish-larva, inspired microrobot. We designed + and – ciliary bands on the top and bottom sides, respectively, of the soft robot, as shown in Fig. 2. As the microrobot is released and exposed to ultrasound of 68.8 kHz at 20 Vpp, it exhibits a left-to-right translational propulsion shown in the image sequence of Fig. 2 depicting the microrobot travelling at ~2.6 mm/s (10 body lengths/second).

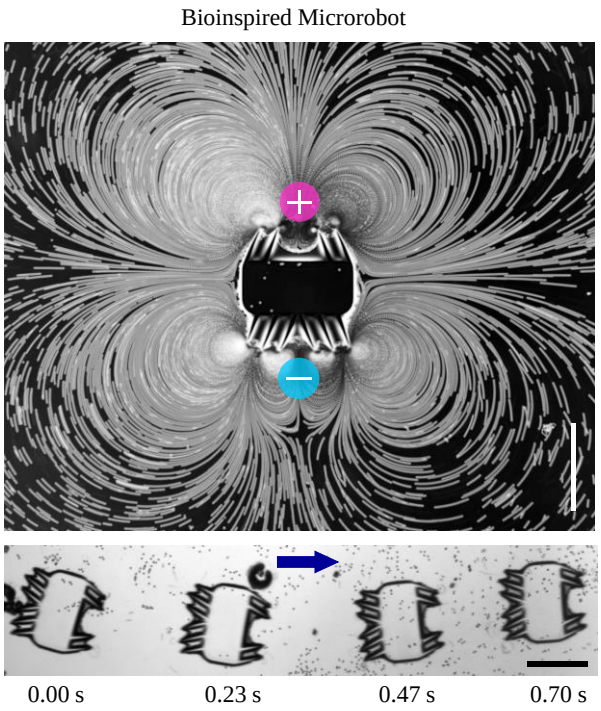

Fig. 2. A starfish-inspired microrobot consisting of a + (top) and a – (bottom) ciliary band placed in a tracer/water solution to visualize acoustic streaming. The superimposed time-lapse image demonstrates controlled translational motion of the microrobot under the application of ultrasound with frequency f = 68.8 kHz at Vpp = 20. Scale bars, 250 µm.

The Reynolds number of the bioinspired microrobot can be estimated as $Re = uD/\nu \approx 0.7$, where u=2.6 mm/s is the swimming velocity, D=280 μm is the width of the microrobot and $\nu \approx 10^{-6}$ m^2/s the water's kinematic viscosity at room temperature. This value also suggests that the system is viscous-dominated and thus must not exhibit any noticeable motion, per the scallop theorem [6]. According to the scallop theorem, the small amplitude and therefore fully reciprocal oscillations of each cilium are not supposed to create net propulsion at the microscale. However, since ultrasound causes the ciliary band to oscillate we must consider the Reynolds number associated with the oscillation of the cilia. For ultrasound actuated systems, the steady flow field is driven by the nonlinear interactions of the harmonic first-order response of the fluid [5]. This can also be deduced from a perturbation expansion approach (see Appendix) where the second-order system of the Navier-Stokes equations is driven by time-averaged nonlinear first-order terms that scale with the frequency Reynolds number (Re_f). Depending on Re_f, estimated as $Re_f = 2\pi f\varepsilon L/\nu \approx 31.4 - 62.8$, where f=100 kHz is the excitation frequency and ε≈0.5-1.0 μm is the oscillation amplitude, these terms can introduce sufficient inertia in the system to achieve swimming, even for reciprocal motion, rendering the Scallop theorem here, as inapplicable.

C. Microparticle Transport

Here, we introduce a microparticle trapping strategy inspired by the feeding mechanism of a starfish larvae [1]. Briefly, this mechanism is characterized by the juxtaposition of ciliary arrays that beat in reverse, generating a specific flow field that facilitates the transport of particles and nutrients to the larva's surface for subsequent capture. Correspondingly, we design an analogous structure that incorporates a combinatorial arrangement of + and – ciliary bands, as shown in Fig. 3(a).

When a synthetic band with this arrangement is exposed to ultrasound, microparticles in close vicinity of the ciliary band are attracted to and travel left-to-right along the ciliary arrangement. At the center of the + ciliary band, the microparticles are pushed away by the fluid source-like streaming. Given that the strength of the source diminishes with distance from the + ciliary band, the effect of the adjacent sink becomes more prominent as the microparticles progress, causing them to be transported towards the – ciliary band. Overall, this arrangement of adjacent + and – ciliary bands allows the migration of microparticles from one ciliary band to another. Combined with an efficient capture strategy this power-controllable transport mechanism, as demonstrated in Fig. 3(b), can be used to design efficient microrobotic systems that can attract and capture particles of interest from the surrounding flow field.

III. Discussion

At the microscale, fluids are associated with low Reynolds number, inertial effects are negligible; microorganisms living in such an environment must have their cilia produce a non-linear whip-like motion, i.e. an asymmetric beat pattern, in order to overcome the reversibility of the flow fields. Our soft ultrasound ciliary bands are distinct from biological cilia in that

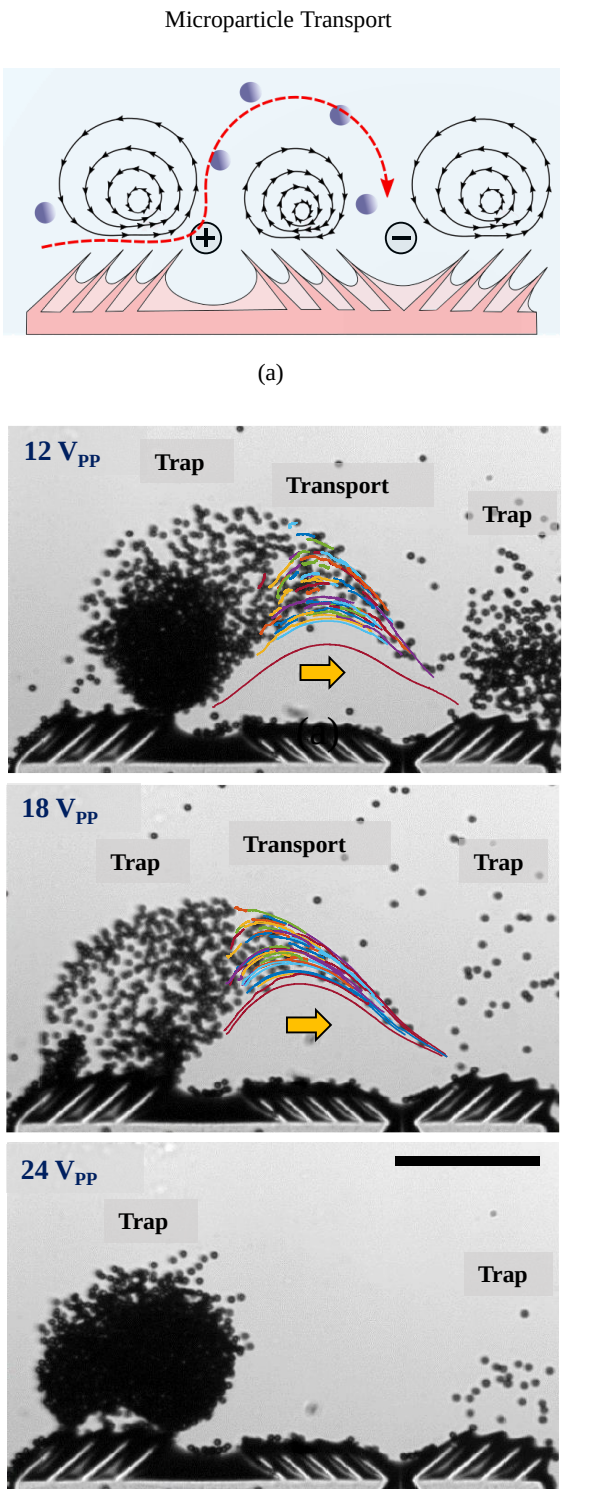

Fig. 3. Bioinspired microparticle trapping using a combination of + and – ciliary bands. (a) Schematic of the transport and trapping mechanism consisting of a + ciliary band adjacent to a – ciliary band. (b) Acoustic power-dependent transport and trapping of 10 μm particles with maximum transport efficiencies at 12 and 18 Vpp, whereas at 24 Vpp the trapping mode becomes dominant. Scale bar, 200 μm.

they produce flow through reciprocal motion, the success of which can be attributed to frequency at which they oscillate at least three orders of magnitude higher than achieved by their biological counterparts. We believe the present work introduces a new design space for externally-actuated field-driven microrobotics and the engineering of cilia and ciliary bands. We look forward to studying the performance of our ultrasound-based ciliary bands in terms of fluid flow, propulsion, and particle transport near walls and in confined channels in biologically-relevant fluid mediums under physiologically-relevant conditions, including non-pulsatile and pulsatile flow. Currently, the angle of our ciliary bands are fixed, we plan that a light-activated liquid crystal polymer can be used to dynamically change the orientations of ciliary bands, i.e. switch from + to – arrangements and vice versa, thereby enabling the development of a robotic system that closely mimics its natural counterparts in propulsion and feeding (trapping) mechanisms. Finally, the concept of + and – ciliary bands can be utilized in lab-on-a-chip systems to realize label-free trapping, fluid mixing, pumping at low Reynolds fluid low, and separation of particles for portable diagnostics applications.

APPENDIX

The perturbation approach expresses the fluid response to acoustic actuation as a sum of the first-order harmonic fields of the Navier-Stokes equations $(\mathbf{v_1}, \mathrm{p}_1, \rho_1)$ and the second-order steady fields $(\mathbf{v}_2, \mathrm{p}_2, \rho_2)$, e.g., $\mathbf{v} = \varepsilon\mathbf{v_1} + \varepsilon^2\mathbf{v_2} + \cdots$, where ε is an appropriate smallness parameter [7]. This approach represents the steady flow field induced by the ciliary bands of the microrobot in a fluid by a second-order system of equations $(\mathbf{v}_2, \mathrm{p}_2, \rho_2)$, which, in turn, is driven by the body force and mass source terms stemming from nonlinear interactions of the time-harmonic first-order fields $(\mathbf{v_1}, \mathrm{p}_1, \rho_1)$. The first-order fluid response is represented by the linearized Navier-Stokes equations, and can be expressed in terms of the non-dimensional frequency Reynolds number. We begin by defining the following non-dimensional quantities:

$$\hat{\rho} = \frac{\rho_0}{\tilde{\rho}}, \quad \hat{\mathbf{v}}_\mathbf{1} = \frac{\mathbf{v_1}}{\tilde{\mathrm{v}}}, \quad \hat{\mathrm{t}} = \frac{\mathrm{t}}{\tilde{\mathrm{t}}}, \quad \hat{\mu} = \frac{\mu}{\tilde{\mu}}, \qquad (1)$$

where $\tilde{\rho}, \tilde{\mathrm{v}}, \tilde{\mathrm{t}}$ and $\tilde{\mu}$ denote the characteristic scales for the first-order velocity, density, time, and viscosity, respectively. Using these non-dimensional quantities, the first-order momentum equation can be expressed as

$$\mathrm{Re}_f \hat{\rho} \frac{\partial \hat{\mathbf{v}}_\mathbf{1}}{\partial \hat{\mathrm{t}}} = -\hat{\nabla}\hat{\mathrm{p}}_1 + \hat{\mu}\hat{\nabla}^2\hat{\mathbf{v}}_\mathbf{1} + \left(\hat{\mu}_\mathrm{b} + \frac{1}{3}\hat{\mu}\right)\hat{\nabla}\left(\hat{\nabla}.\hat{\mathbf{v}}_\mathbf{1}\right), \qquad (2)$$

where, as expected, the relative strength of the inertial and viscous terms at the first-order is characterized by the frequency Reynolds number given as $\mathrm{Re}_f = \frac{\tilde{\rho}\tilde{\mathrm{v}}\tilde{\mathrm{L}}}{\tilde{\mu}}$, with $\tilde{\mathrm{L}}$ being the characteristic length scale for the first-order system. Noting that the first-order (actuation) velocity scale can be expressed as $\tilde{\mathrm{v}} = \omega\Delta\mathrm{s} = 2\pi f\Delta\mathrm{s}$ and denoting kinematic viscosity as $\nu = \frac{\tilde{\mu}}{\tilde{\rho}}$, the frequency Reynolds number can be expressed as $\mathrm{Re}_f = 2\pi f\Delta s\mathrm{L}/\nu$.

Next, we consider the relative strength of the forcing term in the second-order momentum equation (eq. 3) with respect to the viscous terms.

$$\rho_0\left\langle\frac{\partial \mathbf{v_2}}{\partial \mathrm{t}}\right\rangle + \left\langle\rho_1\frac{\partial \mathbf{v_1}}{\partial \mathrm{t}}\right\rangle + \rho_0\langle(\mathbf{v_1}.\nabla)\mathbf{v_1}\rangle = -\nabla\mathrm{p}_2 + \mu\nabla^2\mathbf{v_2} + (\mu_\mathrm{b} + \frac{1}{3}\mu)\nabla(\nabla.\mathbf{v_2}) \qquad (3)$$

Specifically, the third term on the left-hand side of eq. 3 scales as $\rho_0\langle(\mathbf{v_1}.\nabla)\mathbf{v_1}\rangle \sim \frac{\tilde{\rho}\tilde{\mathrm{v}}^2}{\tilde{\mathrm{L}}}$, while the viscous term in eq. 3 scales as $\mu\nabla^2\mathbf{v_2} \sim \frac{\tilde{\mu}\tilde{\mathrm{v}}_\mathrm{s}}{\tilde{\mathrm{L}}_\mathrm{s}^2}$. Therefore, the relative strength of the forcing term with respect to the viscous terms is given by the ratio

$$\frac{\tilde{\rho}\,\tilde{\mathrm{v}}^2}{\tilde{\mathrm{L}}}.\frac{\tilde{\mathrm{L}}_\mathrm{s}^2}{\tilde{\mu}\,\tilde{\mathrm{v}}_\mathrm{s}} \quad \sim \quad \mathrm{Re}_f\frac{\tilde{\mathrm{v}}}{\tilde{\mathrm{v}}_\mathrm{s}}\left(\frac{\tilde{\mathrm{L}}_\mathrm{s}}{\tilde{\mathrm{L}}}\right)^2 \quad \sim \quad \mathrm{Re}_f\frac{\tilde{\mathrm{v}}_\mathrm{s}}{\tilde{\mathrm{v}}}\left(\frac{\tilde{\mathrm{t}}_\mathrm{s}}{\tilde{\mathrm{t}}}\right)^2 \qquad (4)$$

where $\tilde{\mathrm{v}}_\mathrm{s}, \tilde{\mathrm{L}}_\mathrm{s}$, and $\tilde{\mathrm{t}}_\mathrm{s}$ denote the characteristic scales for the streaming velocity, length, and time, respectively. Thus, the forcing term in the second-order system depends on the frequency Reynolds number as well as the separation of time and length (or velocity) scales between the first-order and the streaming flow.

REFERENCES

[1] W. Gilpin, V. N. Prakash, and M. Prakash, "Vortex arrays and ciliary tangles underlie the feeding-swimming trade-off in starfish larvae," *Nat. Phys.*, vol. 13, no. 4, pp. 380–386, 2017, doi: 10.1038/nphys3981.

[2] E. Milana, B. Gorissen, S. Peerlinck, M. De Volder, and D. Reynaerts, "Artificial soft cilia with asymmetric beating patterns for biomimetic low-Reynolds-number fluid propulsion," *Adv. Funct. Mater.*, vol. 29, no. 22, p. 1900462, 2019.

[3] X. Zhang, J. Guo, X. Fu, D. Zhang, and Y. Zhao, "Tailoring Flexible Arrays for Artificial Cilia Actuators," *Adv. Intell. Syst.*, p. 2000225, 2020.

[4] H. Schlichting and K. Gersten, *Boundary-Layer Theory*. Springer Berlin Heidelberg, 2016.

[5] N. Nama, P. H. Huang, T. J. Huang, and F. Costanzo, "Investigation of acoustic streaming patterns around oscillating sharp edges," *Lab Chip*, 2014, doi: 10.1039/c4lc00191e.

[6] E. M. Purcell, "Life at low Reynolds number," *Am. J. Phys.*, 1977, doi: 10.1119/1.10903.

[7] S. S. Sadhal, T. Laurell, and A. Lenshof, "Analysis of acoustic streaming by perturbation methods," in *Microscale Acoustofluidics*, Royal Society of Chemistry London, 2014, pp. 256–311.